RSC Advances

PAPER

View Article Online
View Journal | View Issue

Cite this: *RSC Adv.*, 2015, **5**, 44943

Fabrication, characterisation and *in vitro* biological activities of a sulfuretin-supplemented nanofibrous composite scaffold for tissue engineering

YoungWon Koo,[a] Hyeongjin Lee,[a] Suji Kim,[b] No-Joon Song,[b] Jin-Mo Ku,[c] JaeHwan Lee,[b] Chang Hyun Choi,[a] Kye Won Park[b] and GeunHyung Kim*[a]

Received 14th April 2015
Accepted 13th May 2015

DOI: 10.1039/c5ra06648d

www.rsc.org/advances

Electrospun micro/nanofibrous scaffolds are widely used in various tissue regeneration applications because they have a similar structure to the extracellular matrix and can induce high attachment, proliferation and even differentiation of cultured cells. Here, we designed a new composite scaffold consisting of poly(ε-caprolactone) (PCL), bone morphogenetic protein (BMP-2) and sulfuretin fabricated using a combined process, *i.e.* electrospinning/plasma-treatment/coating. In the composite, we introduced a new bioactive component, sulfuretin, which was used as a cell stimulant to regenerate bone tissue. Sulfuretin release from the composite was controlled by coating of a fixed concentration of alginate. The *in vitro* biocompatibilities of the fibrous composites were examined using preosteoblasts (MC3T3-E1s), and the composite showed high cell adhesion and differentiation for a limited range of sulfuretin compared to the control, which lacked sulfuretin. These results suggest sulfuretin to be an effective supplemental bioactive agent for enhancing bone tissue growth on fibrous composite scaffolds.

Introduction

The ultimate object of tissue engineering, an interdisciplinary field of study that combines engineering, material science and cell biology, is to regenerate injured tissues and organs by using biocompatible porous materials that mimic the original native tissue.[1,2] For successful regeneration of tissues, various fabrication methods have been used—including *e.g.* electrospinning,[3] gas foaming,[4] solid free-form fabrications,[5] and salt leaching.[6,7] Of these methods, electrospinning is widely used to produce micro/nanofibres, which have a similar physical structure to the extracellular matrix (ECM) and a high surface-to-volume ratio. These physical structures of the micro/nanofibres can provide biological cues to the cells, resulting in successful regeneration of various tissues.[8]

The synthetic polymer poly(ε-caprolactone) (PCL) has been extensively used in fabricating bioscaffolds because it shows easily controllable degradability; moreover, it is nontoxic and exhibits easy and versatile processability and possesses considerable mechanical properties compared to natural biopolymers.[9,10] However, like the most synthetic biopolymers, the PCL absences cell adhesive motifs—proteins and peptides such as fibronectin binding to integrin and Arg-Gly-Asp (RGD) peptide—to induce high cell adhesion, growth and differentiation.[11] To overcome the low cell-activating or -stimulating functions of the synthetic polymer, we designed a new biocomposite system supplemented with bone morphogenetic protein (BMP-2) and sulfuretin. BMPs belong to the transforming growth factor-β (TGF-β) superfamily, which can control cell migration, proliferation, and even differentiation and angiogenesis.[12,13] Since BMP-2 of the BMPs is one of the significantly important signalling molecules in bone formation, it has been widely used as an imperative osteoinductive material.[14–17]

Sulfuretin can be extracted from *Rhus verniciflua* Stokes (RVS; the lacquer tree native to East Asia) and has been subjected to evaluation of medical properties, such as antihuman cancer,[18–20] anti-inflammatory,[21,22] antileukaemia,[19] antimutagenic,[23] antiplatelet,[24] and anti-rheumatoid arthritis[25] effects. Although sulfuretin has shown exceedingly positive effects as a medical assisting and/or treating component, it has not been used in tissue regenerative material, in particular as a bioactive component for bone regeneration. Moreover, sulfuretin has not been combined in any composite system as a dispersed bioactive material supplemented to the nanofibrous structure.

In this study, we designed a new composite system that used various concentrations of sulfuretin/alginate coated onto PCL/BMP-2 electrospun fibres. The function of BMP-2 powder, which was composed of rhBMP-2 coated on β-TCP (β-tricalcium phosphate) and hydroxyapatite (HA) granules, in the composite was to enhance the mechanical properties and osteogenesis.[26] To effectively control its function, sulfuretin release from the composite scaffolds was controlled by coating with a fixed

[a]*Department of Biomechatronic Eng., Sungkyunkwan University, Suwon 440-746, Korea. E-mail: gkimbme@skku.edu; Tel: +82 31 2907828*

[b]*Department of Food Science and Biotechnology, Sungkyunkwan University, Suwon 440-746, Korea*

[c]*Gyeonggi Bio-Center, Suwon 443-270, Korea*

concentration (20 wt%) of alginate. In general, alginate, an anionic polysaccharide commonly present in the cell walls of brown algae, has been used in drug-delivery systems as a controllable drug-releasing material due to its rapid gelation upon addition of divalent cations (Ca^{2+}).[27,28] In addition, because the alginate has outstanding physiochemical properties such as being nontoxic and nonallergic, it has been applied extensively as a bioink for cell printing, in wound dressings and as a tissue regenerative material.[29] Recently, Liu *et al.* fabricated alginate struts (diameter ≈ 20 μm) that incorporated nanocapsules, which are drug-encapsulated alginate beads. The alginate-based nanocapsules enabled manipulation of drug release.[30]

By using a combined processing method ((1) electrospinning of PCL/BMP-2, (2) plasma-treatment of the electrospun fibres and (3) coating of sulfuretin and alginate), we generated a novel composite material. MC3T3-E1 cells were used to assess the *in vitro* responses of cells on the composite scaffold, including proliferation determined by MTT assay, live/dead cell staining, ALP activity, Runx2 expression and Alizarin Red S (ARS) staining. Furthermore, sulfuretin release over time and the physical properties, water contact angle (WCA), biodegradation and mechanical properties of the composite scaffolds were determined.

Materials and methods

Materials

A PCL solution was generated by dissolving 10 wt% PCL (M_w = 80 000 g mol^{-1}; Sigma-Aldrich, St. Louis, MO, USA) in methylene chloride/dimethyl formamide (MC/DMF) solvent (a mixture of methylene chloride (Junsei, Tokyo, Japan) and dimethylformamide (Junsei) in a 4 : 1 ratio). BMP-2 powder (mixture of rhBMP-2, β-TCP, and HA, Cowellmedi, Busan, South Korea) was mixed with the PCL solution at 0.5 wt% to fabricate nanofibres. Alginate solution for coating on the electrospun PCL/BMP-2 fibres was prepared by dissolving 20 wt% G-content nonmedical grade LF10/60 alginate (FMC BioPolymer, Drammen, Norway) in triple-distilled water. To cross-link the alginate solution, $CaCl_2$ (Sigma-Aldrich) was used. Sulfuretin (M_w = 270.241 g mol^{-1}), kindly provided by Dr Ku of Gyeonggi Bio-Center (Suwon, South Korea), was obtained by extraction from RVS using ethanol. Fig. 1(a–d) shows optical and scanning electron microscopy (SEM) images and the chemical structure of sulfuretin and BMP-2 powder, respectively. We used 70% (v/v) ethanol to dissolve the sulfuretin powder; the sulfuretin concentrations used were 0.5, 1, 5 and 10 mM.

Preparation and chemical identification of sulfuretin

To a mixture of 3.74 g (24.9 mmol) of methyl 6-hydroxybenzofuran-3(2*H*)-one and 3.44 g (24.9 mmol) of 3,4-dihydroxybenzaldehyde in ethanol (124 mL), 12 N HCl (37.4 mL) was added drop-wise at 0 °C. Then the reaction mixture was reacted at 60 °C until the reaction was finished from TLC monitoring. The mixture was poured into water and the resulting precipitate was filtered and dried in vacuum. The crude product was recrystallized by $MeOH/H_2O$ to yield 5.38 g (80.0%) of sulfuretin as a yellow powder. The synthesized sulfuretin was identified by LC/MS (Fig. 1(e and f)). LC was performed on WATERS ACQUITY UPLC BEH C18 column (2.1 × 100 mm; Milford, MA, USA). The mobile phase A was 0.1% formic acid in water and

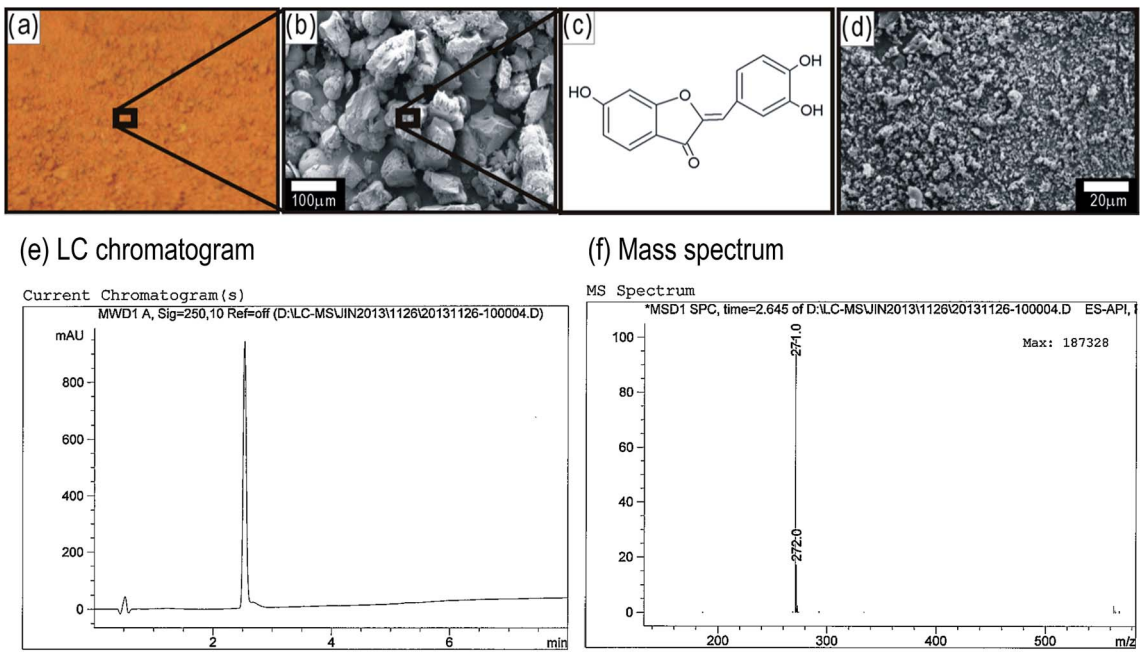

Fig. 1 (a) Optical and (b) SEM images of sulfuretin powder. (c) The molecular structure of sulfuretin. (d) A SEM image of BMP-2 powder, which was composed of rhBMP-2 coated on β-TCP/HA granules. (e) Liquid chromatography was performed on C18 column (2.1 × 100 mm) (mobile phase: phase A: 0.1% formic acid in water, phase B: 0.1% formic acid in acetonitrile). (f) Positive ion mass spectrum was generated using a Micromass Quattro Micro API mass spectrometer. Protonated sulfuretin $[M + H]^+$ was detected at a retention time of 2.64 min.

phase B was 0.1% formic acid in acetonitrile. Mass spectrum was performed with Micromass Quattro Micro API mass spectrometer (Milford, MA, USA). The monoisotopic mass of protonated sulfuretin $[M + H]^+$ was detected at a retention time of 2.64 min.

Fabrication of PCL/BMP-2/sulfuretin/alginate fibrous composites

To obtain nanofibres of PCL/BMP-2, the mixed PCL/BMP-2 solution was placed in a 10 mL syringe with a 16 G needle. The flow rate of the solution (0.5 mL h^{-1}) was controlled by a syringe pump system (KDS 230, KD Scientific, Ansan, South Korea). A high-voltage power supply (HVDC, SHV300RD-50K, Convertech, Suwon, South Korea) was used and the applied electric field was set at 1.2 kV cm^{-1} to obtain nanofibres.

Because the electrospun PCL/BMP-2 nanofibres were hydrophobic, the fibrous mats were treated with oxygen plasma using low-frequency plasma (CUTE-MP/R, Femto-Science, Inc., Busan, South Korea) for 5 min. A frequency of 50 kHz, a power of 50 W and a pressure of 5.3×10^{-1} Torr were used.

The plasma-treated fibrous mats were dipped in 0.5, 1, 5 and 10 mM sulfuretin solutions for 2 h, and each coated fibrous mat was dried and re-coated with 20 wt% alginate solution by dipping. Then, the coated alginate was cross-linked in 10 wt% $CaCl_2$ solution for 10 min and washed with phosphate-buffered saline (PBS) three times to eliminate $CaCl_2$ from the fibrous composites. The amount of coated alginate on the fibrous mat was determined by weighing fiber mats before and after the coating process. 0.6 ± 0.01 mg of alginate was coated per fibrous mat (diameter = 5 mm and thickness = 0.13 mm) (n = 10). The composite scaffold fabrication procedure is shown in Fig. 2(a–e).

Characterisations of the composite scaffolds

The WCAs for five independent samples were averaged and are presented as the means ± SD. Water (10 μL) was placed on the surface of the composite scaffolds, and after 1 min the WCA was measured under an atmospheric temperature of 26 °C and humidity of 37%.

To assess the degradation of the composite scaffolds, the initial weight (W_i) was measured. The composite scaffolds were then immersed in PBS (pH 7.4) containing lysozyme (10 000 U mL^{-1}) at 37 °C. After incubation for various time periods, the samples were rinsed with deionised water and freeze-dried,

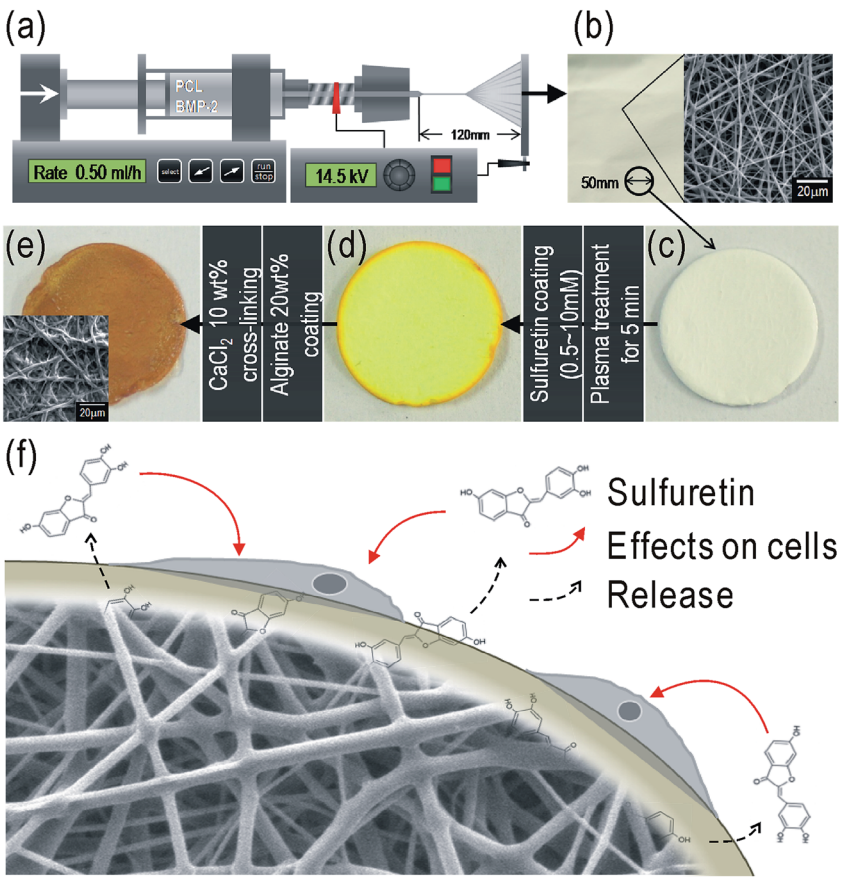

Fig. 2 Schematic of fabrication of the PCL/BMP-2/sulfuretin/alginate composite scaffolds. (a and b) The PCL/BMP-2 fibres were deposited on a collecting plate *via* electrospinning process and cut into 5 mm diameter round pieces. (c and d) To enhance their hydrophilicity, the composite of the PCL/BMP-2 fibres was treated with oxygen plasma for 5 minutes and the plasma-treated composites were coated with 0.5, 1, 5 or 10 mM sulfuretin for 2 h. (d and e) The sulfuretin-coated fibrous composite was coated with 20 wt% alginate, and the coated alginate was cross-linked with $CaCl_2$ solution (10 wt%). (f) A schematic of the effect of alginate coating for the release of sulfuretin from the composite scaffolds.

after which their weight (W_f) was measured. The per cent weight loss was calculated with the following equation: weight loss (%) = $[(W_i - W_f)/W_i] \times 100$. Weight loss is shown as the mean ± SD of five samples.

The mechanical properties of samples were determined using a micro-tensile tester (Toptech 2000, Chemilab, Seoul, South Korea) in tensile mode. Samples 5 × 20 mm (width × length) in size were prepared. The thickness of the samples was measured at three points under an optical microscope and the values were averaged. The tensile test was performed in a "dry" state. The samples were stretched to failure at a stretching speed of 1 mm s^{-1} at room temperature. All values are expressed as means ± standard deviation ($n = 5$).

Sulfuretin release test

Sulfuretin released from the composites was monitored by UV-spectrophotometry (Optizen 2120UVPlus, Mecasys Co., Daejeon, South Korea) in PBS (pH 7.4) at a wavelength of 405 nm. The sulfuretin release test was carried out by incubating the scaffold in 15 mL of PBS solution at 37 °C. The scaffold was incubated in PBS solution for various periods. To measure sulfuretin release, 1 mL of the 15 mL of release solution was extracted and tested for the drug; the aliquot was then returned to the release solution. To avoid contamination of release solution, the pipette tip and cuvette of the spectrophotometer were sterilised with 70% ethanol. The cumulative amount of sulfuretin released was calculated as a function of time.

The total amount of sulfuretin coated in the fibrous mats, which were not dipped in alginate solution, was measured using a standard curve using the spectrophotometry. To obtain the standard curve, we measured the optical density for 20, 40, 60, 80, and 100 μM sulfuretin. A good linearity (correlation coefficient of 0.999) for the standard plot of the optical density *versus* sulfuretin concentrations ranging from 20 to 100 μM was obtained. The sulfuretin concentrations released from the fibrous mats, which were dipped in 0.5, 1, 5 and 10 mM sulfuretin solutions, were determined using the UV-spectrophotometer at 405 nm and evaluated in triplicate. The released solution was taken at 2 days, and PBS at 37 °C was used as the dissolution medium.

In vitro cell culture

The composite scaffolds were sterilised with 70% ethanol and ultraviolet (UV) light, and then placed in culture medium overnight. Mouse preosteoblast cells (MC3T3-E1; ATCC, Manassas, VA, U.S.A.) were used to evaluate the behaviour of cells cultured on the scaffolds. The cells were cultured for up to four passages in 24-well plates containing α-minimum essential medium (α-MEM, Life Technologies, Carlsbad, CA, U.S.A.) with 10% foetal bovine serum (Gemini Bio-Products, West Sacramento, CA, U.S.A.) and 1% penicillin/streptomycin (Cellgro, Mediatech, Manassas, VA, U.S.A.) for a concentration of 100 IU mL^{-1} penicillin and 100 μg mL^{-1} streptomycin.

The cells were collected by trypsin–ethylenediaminetetraacetic acid (EDTA) treatment, seeded onto the scaffolds at a density of 1×10^5 per sample and incubated at 37 °C in an atmosphere of 5% CO_2.

Cell proliferation was examined by the MTT (3-(4,5-dimethylthiazol-2-yl)-2,5-diphenyl tetrazolium bromide) assay (Cell Proliferation Kit I, Boehringer Mannheim, Mannheim, Germany) after cell culture for 1, 3 and 7 days. Cells/scaffolds were incubated with MTT (0.5 mg mL^{-1}) for 4 h at 37 °C and the absorbance at 570 nm was measured using a microplate reader (EL800, Bio-Tek Instruments, Winooski, VT, U.S.A.). Five samples were used for each incubation period and each test was performed in triplicate.

Live/dead cell staining

The scaffolds were exposed to 0.15 mM calcein AM and 2 mM ethidium homodimer-1 for 45 min in an incubator (after culture for 1, 3 and 7 days) to observe live and dead cells. The analysis was performed under a microscope (TE2000-S, Nikon, Tokyo, Japan) equipped with an epifluorescence attachment and a SPOT RT digital camera (SPOT Imaging Solutions, Sterling Heights, MI, U.S.A.). We captured images and processed the area of green spots using the ImageJ software (NIH, Bethesda, MD, U.S.A.) to assess the percentage of live cells.

DAPI/phalloidin staining

After 7 and 14 days of cell culture, the composite scaffolds were subjected to diamidino-2-phenylindole (DAPI) fluorescent staining to detect cell nuclei. Phalloidin (Invitrogen, Carlsbad, CA, U.S.A.) staining was performed to visualise the actin cytoskeleton of proliferated cells. The stained scaffolds were visualised under a microscope (TE2000-S, Nikon, Tokyo, Japan) equipped with an epifluorescence attachment and a SPOT RT digital camera (SPOT Imaging Solutions).

Alizarin Red S (ARS) staining

Mineralisation levels were determined by ARS staining in 24-well plates. MC3T3-E1 cells were cultured in α-MEM and then washed three times with PBS, fixed in 70% (v/v) cold ethanol (4 °C) for 1 h and air-dried. Ethanol-fixed specimens were stained with 40 mM ARS (pH 4.2) for 1 h and washed three times with purified water. Specimens were then distained with 10% cetylpyridinium chloride in 10 mM sodium phosphate buffer (pH 7.0) for 15 min. The optical density (OD) at 562 nm was measured using a Spectra III UV microplate reader (Spectra III, SLT-Lab Instruments, Salzburg, Austria).

Real-time PCR analysis

Total RNAs from MC3T3-E1 cells cultured on scaffolds were extracted using TRIzol reagent (Invitrogen, Carlsbad, CA, U.S.A.) as described previously.[31] Briefly, total RNAs were extracted and 0.5 μg was subjected to reverse transcription to synthesise complementary DNAs (cDNAs) using RTase M-MLV (2640A, TaKaRa, Ohtsu, Japan). Expression of alkaline phosphatase (ALP) and Runx2 was measured using Power SYBR Premix Ex Taq (RP041A, TaKaRa) with gene-specific primer sets in a thermal cycler (TaKaRa). The gene-specific forward and reverse

oligonucleotide primer sets were synthesised by Integrated DNA Technologies (San Diego, CA, U.S.A.). The following gene-specific primers were used for real-time PCR: ALP F (accession #: NM_007431), 5′-AAACCCAGAACACAAGCATTCC-3′, ALP R, 5′-ACCAGCAAGAAGAAGCC-3′; 36B4 F (accession #: NM_007475), 5′-AGATGCAGCAGATCCGCAT-3′, 36B4 R, 5′-GTTCTTGCCCAT CAGCACC-3′; Runx2 F (accession #: NM_001145920), 5′-GCCCAGGCGTATTTCAGA-3′, Runx2 R, 5′-TGCCTGGCTCTTC TTACTGAG-3′. The relative expression levels (fold change) were obtained using the $2^{-\Delta CT}$ method and normalised to the levels of 36B4.

Statistical analysis

All data are presented as means ± SD. Statistical analyses were performed using the SPSS software (ver. 20.0, SPSS, Inc., Chicago, IL, U.S.A.) and consisted of single-factor analyses of variance (ANOVAs). In all analyses, $p < 0.05$ was considered to indicate statistical significance.

Result and discussion

Stimulatory effects of sulfuretin on osteoblastic differentiation in MC3T3-E1 cells

To test the pro-osteogenic effects of the sulfuretin, MC3T3-E1 cells were exposed to sulfuretin for 10 days and its effects on osteoblast differentiation were assessed. An osteoblast marker, alkaline phosphatase (ALP) activity was measured to examine the effects on osteoblast differentiation (Fig. 3(a)). Treatments of sulfuretin at 10–20 μM strongly increased ALP activity with a modest induction at 30 μM suggesting the pro-osteogenic actions of sulfuretin. Expression of genes linked to osteoblast differentiation was further measured to confirm the actions of sulfuretin in osteogenesis (Fig. 3(b)). Consistent with increased ALP activity, real time PCR analysis showed that sulfuretin at 20 μM stimulated the expression of genes encoding osteocalcin (OCN), colagen I (Col I), osterix, and Runx2 compared to control treatment. Therefore, ALP activity and gene expression analyses show the sulfuretin derived from natural herbal products can act as an osteoinductive factor.

Preparation of PCL/BMP-2/sulfuretin/alginate fibrous composite using electrospun PCL/BMP-2 fibres

In the electrospinning process, we used an auxiliary cylindrical electrode connected to the spinning nozzle to stabilise the initial jet zone by concentrating the electric field in the spinning axis.[32] Fig. 4(a) shows the initial spun jet and whipped/stretched micro/nanofibres using PCL/BMP-2 solution (electrical conductivity = 6.47 μS cm^{-1}; surface tension = 0.034 N m^{-1}). Fig. 4(b) shows an SEM image of PCL/BMP-2 fibres with diverse diameters. In Fig. 4(c), the diameters of PCL/BMP-2 nano/microfibres were found to be distributed in two diameter ranges (0.5–2.5 μm and 3.5–6.5 μm), which is termed a bimodal distribution. Deitzel *et al.* first investigated a bimodal fibrous

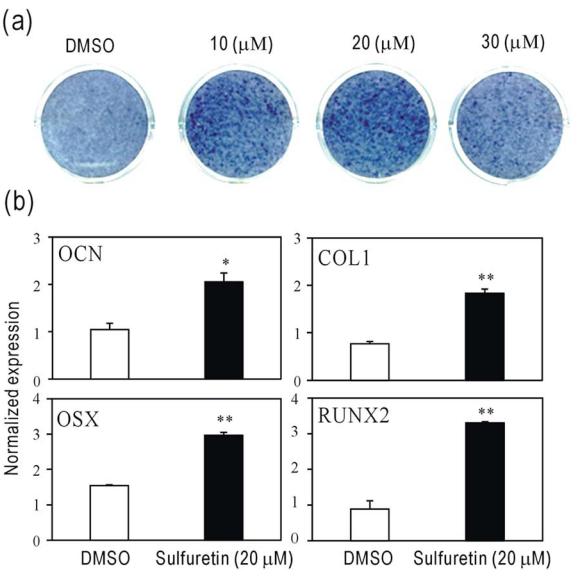

Fig. 3 (a) MC3T3-E1 cells were treated with sulfuretin for 10 days and ALP-positive cells were stained. (b) MC3T3-E1 cells were treated with sulfuretin at the indicated doses for 10 days and relative expression of osteocalcin (OCN), collagen I (Col I), osterix (OSX), and Runx2 mRNA were determined by real-time polymerase chain reaction. Data are means standard deviations from three independent experiments (*$p < 0.05$, **$p < 0.005$).

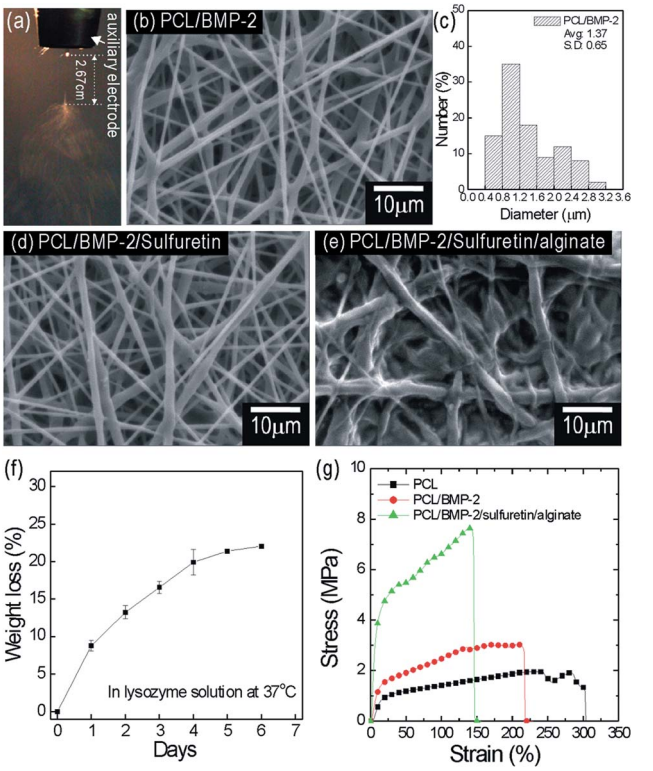

Fig. 4 (a) Whipped/stretched fibres in PCL/BMP-2 solution during the electrospinning process, and (b) SEM image and (c) size distribution of electrospun PCL/BMP-2 fibres. SEM images of (d) sulfuretin-coated PCL/BMP-2 fibres and (e) an alginate-coated PCL/BMP-2/sulfuretin composite scaffold. (f) Weight loss of PCL/BMP-2/sulfuretin/alginate scaffolds for the indicated time periods. (g) Stress–strain curves for the PCL, PCL/BMP-2 and PCL/BMP-2/sulfuretin/alginate scaffolds.

structure using an electrospinning process.[33] Although this bimodal structure is still under investigation in terms of the exact relationship between the bimodal form and cell proliferation,[34] bimodal fibres with a nano- and microscale hierarchical structure can induce various cellular activities.[35–38] For this reason, we can estimate that the bimodal topological structure of the PCL/BMP-2 fibres would enhance cellular activities compared to homogeneous structural fibres. Following their fabrication sulfuretin was coated on the PCL/BMP-2 fibres. However, because the fibres are hydrophobic (WCA = 115 ± 2.6°), they were treated with an oxygen plasma to increase their hydrophilicity. After 5 min of plasma treatment, the WCA of the PCL/BMP-2 fibres was 10 ± 1.4°. Four sulfuretin concentrations of 500 μM, 1 mM, 5 mM and 10 mM were used to coat the fibrous PCL/BMP-2 composite. Finally, to control sulfuretin release, 20 wt% alginate was used, based on our previous work.[27] In that study, rhodamine was used as the releasing agent and 5, 10 and 20 wt% alginate were coated onto porous collagen scaffolds. The results showed that coating with 20 wt% alginate showed the most appropriate controllability of rhodamine release from the scaffold. Fig. 4(d and e) shows SEM images of PCL/BMP-2/sulfuretin (10 mM) fibres (PBA) and a PCL/BMP-2/sulfuretin (10 mM)/alginate composite scaffold (PBSA). The amount of sulfuretin coated was measured using a standard curve. The amount of sulfuretin coated on the composite scaffolds, which were dipped in 0.5, 1, 5 and 10 mM sulfuretin solutions, was 12.66 ± 0.65, 20.24 ± 2.15, 59.54 ± 7.83 and 103.51 ± 1.67 μM, respectively. In this work, the scaffolds coated using 0.5, 1.0, 5.0 and 10.0 mM sulfuretin were labelled PBSA-1, PBSA-2, PBSA-3 and PBSA-4, respectively.

Characterisation of PBSA fibrous composite

In general, the hydrophilic property of biomedical substitutes is related to cell growth, migration and physiological responses.[39] The hydrophilicity of the materials was assessed by measuring the WCA. The PBSA-1, -2, -3 and -4 fibrous composite scaffolds showed similar hydrophilic property (WCA = 6.7 ± 1.2° after 1 min).

To assess the biodegradability of the PBSA composites, the weight change was tested for 7 days in lysozyme solution at 37 ± 2 °C. The biodegradation of each PBSA composite scaffold was similar because degradation principally involves the coated alginate (not PCL); therefore, only the PBSA-4 curve is shown (Fig. 4(f)). As revealed in the figure, the degradation of the composite increased linearly with time. The result is directly correlated with sulfuretin release from the composite scaffolds. Based on the degradation curve, sulfuretin was released constantly owing to continuous degradation of the coated alginate.

The mechanical properties of biomedical scaffolds are important parameters for successful regeneration of various tissues because appropriate mechanical properties can maintain the predesigned tissue structure and influence cellular activities.[40] Fig. 4(g) shows the stress–strain curves of the PCL, PCL/BMP-2 and PBSA-4 scaffolds determined using a tensile tester under a 1 mm s^{-1} crosshead speed. The initial slope of the curves was used to calculate the Young's modulus; the moduli of the PCL, PCL/BMP-2 and PBSA-4 were 7.73 ± 1.31 MPa, 12.61 ± 2.37 MPa and 51.16 ± 4.26 MPa, respectively. Therefore, the PBSA scaffold showed greater stiffness compared to the PCL and PCL/BMP-2 scaffolds due to its reinforced alginate component.

Sulfuretin release from the PBSA scaffold

In this study, to interrupt the initial burst of sulfuretin release from the composite scaffolds, we coated the sulfuretin-treated fibrous structure with alginate. Fig. 5(a and b) shows the cumulative percent release for composite scaffolds with (PBSA scaffold) and without (PCL/BMP-2/sulfuretin (PBS) scaffold) an alginate coating, respectively. Sulfuretin release from PBSA scaffolds was inhibited by the alginate coating. In the initial bursts (0–6 h), the sulfuretin release percentage was 0.91% h^{-1} in PBSA scaffolds and 15.70% h^{-1} in PBS scaffolds, which suggests that the initial burst was disturbed by the alginate coating of PBSA composite scaffolds. Moreover, the second burst occurred between days 1 and 5 in PBSA following a time interval of 0.5 days (grey-coloured), which was postulated to be a release-induction phase by Batycky *et al.*[41] This process can be interpreted according to Batycky *et al.* who formulated the process of drug release to determine the amount of released drug over time. According to that study, the mass of the released drug can be formulated using the following equation:

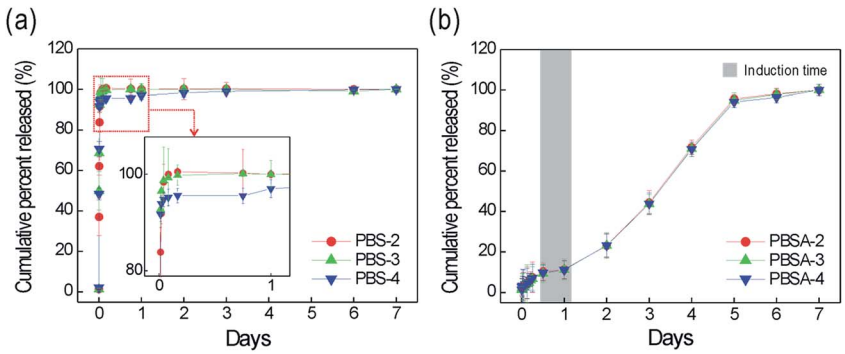

Fig. 5 Cumulative percentage release of sulfuretin from (a) PCL/BMP-2/sulfuretin (PBS) composite scaffolds and from (b) PCL/BMP-2/sulfuretin/alginate (PBSA). The numbers, 2, 3, and 4 indicate the sulfuretin concentrations, 1, 5, and 10 mM, respectively.

$$m_r(t) = m_i\varphi(1 - e^{-k_d t}) \quad (1)$$

where m_i is the initial mass of drug, φ is the mass fraction of the drug involved in the burst relative to the initial drug and k_d is the drug desorption rate constant. The second burst (after induction) can be formulated according to the following equation:[41]

$$\frac{m_d(t)}{m_i} = 1 - \varphi\left(1 - e^{-k_d t}\right) - (1 - \varphi)(1 - \delta(t - t_i)) \quad (2)$$

where δ is directly proportionate to the effective drug diffusivity and inversely to the square of the micro-geometry of the polymer. Based on the result, we can confirm that the sulfuretin release was interrupted effectively by the alginate coating.

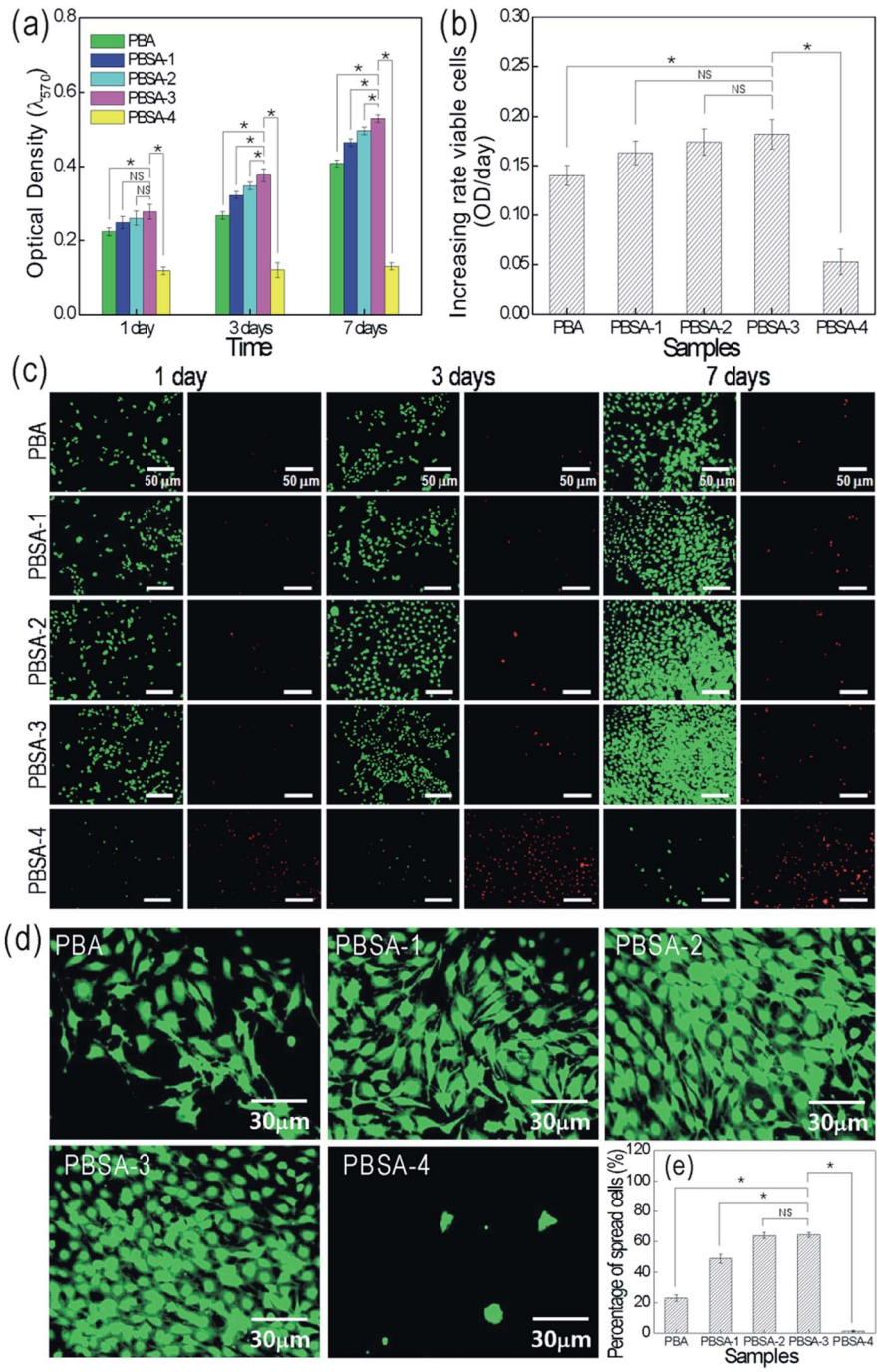

Fig. 6 (a) MTT results and (b) rate of increase in viable cell numbers (slope of optical density of MTT *vs.* culture day) on the composite scaffolds. PBA indicates non-sulfuretin-coated scaffolds and PBSA-1, -2, -3, and -4 indicate the scaffolds with sulfuretin coating concentrations of 0.5, 1, 5, and 10 mM, respectively. (c) Live (green)/dead (red) cells on the indicated composite scaffolds at 1, 3 and 7 days of culture. (d) Magnified image of live cells on the composite scaffolds at 7 days and (e) percentage of spread cells. Asterisks and NS indicate significant and non-significant difference, respectively.

In vitro cell responses

To evaluate the relationship between *in vitro* cell activities and the composite scaffolds with different concentrations of sulfuretin, preosteoblast cells (MC3T3-E1) were cultured on the PBA, PBSA-1, PBSA-2, PBSA-3 and PBSA-4 composite scaffolds. Cell viability is one of the most important parameters for assessing biomedical substitutes as viability can directly affect the final cell responses, such as proliferation and differentiation. In Fig. 6(a), the MTT assay results indicate that the proliferation of viable cells increased on the fibrous composites with increasing culture time and increasing weight fraction of sulfuretin, with the exception of only PBSA-4. In addition, a significant increase in the cell viability rate of the composite scaffolds was observed in the PBSA-3 scaffold for all culture times (Fig. 6(b)). Therefore, the sulfuretin released from the composites facilitates preosteoblast proliferation, but only over a limited range of sulfuretin concentrations.

To qualitatively evaluate live and dead cells on the composite scaffolds, preosteoblasts were stained with calcein AM and ethidium homodimer-1. Fig. 6(c) shows fluorescence images of live (green) and dead (red) cells on composite scaffolds after culturing for 1, 3 and 7 days. As expected from the MTT result, PBSA-3 showed a significantly higher number of viable cells compared to the PBA, PBSA-1 and PBSA-4 scaffolds. After 7 days in culture, the per cent cell spreading was considerably greater on the PBSA-2 and PBSA-3 composite scaffolds than on the PBA and PBSA-4 scaffolds (Fig. 6(d and e)). However, as evidenced by MTT result, the effect of sulfuretin concentration in terms of enhancing cell proliferation was limited.

In Fig. 7(a), the nuclei (blue) and F-actin (red) of preosteoblasts on the PBA, PBSA-1, PBSA-2, PBSA-3 and PBSA-4 scaffolds were examined using fluorescence imaging after culturing for 7 and 14 days. The number of nuclei and cytoskeleton development (actin) were more highly developed on the PBSA-2 and PBSA-3 scaffolds compared to the PBA and PBSA-4 scaffolds (Fig. 7(b and c)). The results indicate that the composite scaffolds supplemented with sulfuretin can induced significant development of the cytoskeleton, but only over a limited range of sulfuretin concentrations.

Generally, ARS is used to evaluate the level of calcium mineral. To assess the effect of sulfuretin, we conducted experiments in which the composite scaffolds were incubated in medium for 7 and 14 days. Fig. 8(a) displays optical images of ARS staining of the composite scaffolds after 7 and 14 days of cell culture. The red colour in the images indicates the area of calcium mineral. As the sulfuretin in the composite scaffolds increased, the density of the red colour rose, indicating an increase in calcium mineralisation, while the PBSA-4 scaffold (highest sulfuretin concentration) showed a significantly reduced area of calcium mineralisation. The optical density (OD) of composite scaffolds extracted from the stained composite scaffolds is shown in Fig. 8(b). The OD value at 14 days was considerably higher than that at 7 days. In addition, as the sulfuretin concentration in the fibrous composites increased, the OD value rose. In particular, the OD value of PBSA-3 at 14 days was almost 2.5-fold that of the control (PBA).

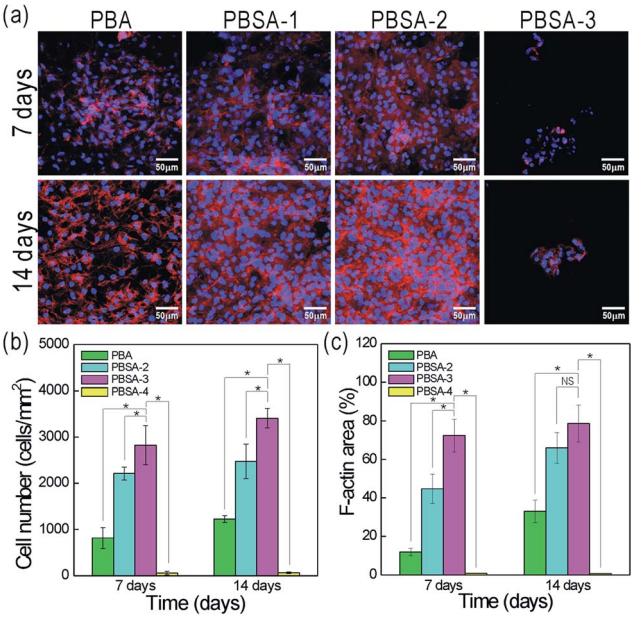

Fig. 7 (a) DAPI (nuclei)/phalloidin (F-actin) images of composite scaffolds after cell culture for 7 and 14 days. (b) Cell number per millimetre squared and (c) F-actin area per cent (%) calculated using images of the composite scaffolds. Asterisks and NS indicate significant and non-significant difference, respectively.

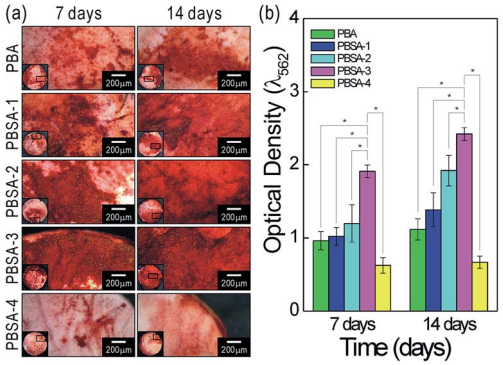

Fig. 8 Calcium mineralisation in MC3T3-E1 cells cultured for 7 and 14 days. (a) Optical images of ARS staining of the composite scaffolds. (b) Optical density of the composites. Asterisks indicate significant differences.

These results are consistent with the optical images of calcium mineralisation. These results propose that conjugation of sulfuretin to nanofibres promoted the osteogenic differentiation of the cells, but only over a limited range of sulfuretin concentrations. These results suggest sulfuretin to be a promising bioactive factor for bone tissue regeneration.

Finally, to confirm the effect of the released sulfuretin from the composite scaffolds on osteogenic differentiation, we measured the expression levels of two osteoblastic markers—ALP and Runx2—using real-time PCR. MC3T3-E1 cells were cultured on PBA (the control scaffold lacking sulfuretin) and PBSA-2 scaffolds for 10 days. As shown in Fig. 9(a), the mRNA expression of ALP increased 2.5-fold in cells grown on the PBSA-

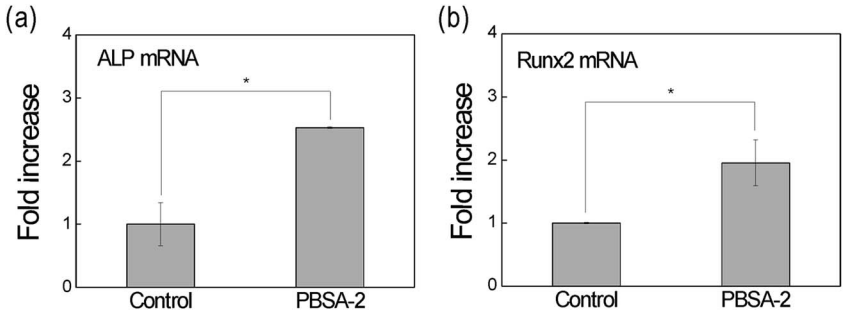

Fig. 9 Effects of sulfuretin scaffolds on osteoblast differentiation. MC3T3-E1 cells were cultured on sulfuretin scaffolds for 10 days, and relative levels of (a) alkaline phosphatase (ALP) and (b) Runx2 mRNA were determined by real-time PCR. Asterisks indicate significant differences.

2 scaffold compared to the control. In addition, mRNA expression of Runx2 was induced approximately 2-fold in cells on the sulfuretin-coated scaffold (Fig. 9(b)). These observations confirm that the released sulfuretin promotes osteoblast differentiation in MC3T3-E1 cells. However, although we showed that the sulfuretin-containing composite scaffolds induce osteoblast proliferation and differentiation, the mechanisms underlying the effect of sulfuretin on preosteoblast cells are unknown. Various signalling pathways modulate the proliferation and differentiation of osteoblasts, including the BMP, TGF-β, Wnt and hedgehog signalling pathways. Therefore, sulfuretin-supplemented scaffolds may plausibly activate one or more of these cascades. In future, it will be interesting to pursue the possibility of sulfuretin as an activator of osteogenic cascades.

Conclusions

Here, a new biocomposite scaffold consisting of nanofibrous PCL/BMP-2 and sulfuretin/alginate was proposed and fabricated using an electrospinning/plasma-treatment/coating process. To ensure continuous biological function of sulfuretin, release of the bioactive component from the composite scaffold was controlled by means of an alginate coating. The composite scaffolds were analysed with regard to a variety of physical and biological activities. The mechanical properties of the composite scaffold were considerably improved compared to the PCL/BMP-2 fibres due to the reinforcing component, *i.e.* alginate. Evaluation of *in vitro* cellular activities using MC3T3-E1 cells demonstrated that the viable cell proliferation and calcium mineralisation levels on the composite scaffold supplemented with sulfuretin were notably enhanced compared to those of the control (PCL/BMP-2 fibrous scaffold). These results suggest that sulfuretin exerts remarkable effects on MC3T3-E1 cells in terms of viability, proliferation and differentiation, but only over a limited concentration range. In conclusion, our data indicate sulfuretin to be an excellent bioactive material for bone tissue regeneration.

Acknowledgements

This study was supported by the Marine Technology Application Program of Ministry of Oceans and Fisheries, Republic of Korea (PJT200673), by the National Research Foundation of Korea (NRF) grant funded by the Korea government (MSIP) (no. 2014R1A2A1A11050047), and also by the Basic Science Research Programme through the National Research Foundation of Korea (NRF) funded by the Ministry of Education, Science and Technology (NRF-2013R1A1A2060447).

References

1 V. Mironov, T. Trusk, V. Kasyanov, S. Little, R. Swaja and R. Markwald, *Biofabrication*, 2009, **1**, 022001.
2 N. G. Rim, C. S. Shin and H. Shin, *Biomed. Mater.*, 2013, **8**, 014102.
3 K. Chatterjee, M. F. Young and C. G. Simon Jr, *Comb. Chem. High Throughput Screening*, 2011, **14**, 227–236.
4 M. Ramalingam, M. F. Young, V. Thomas, L. Sun, L. C. Chow, C. K. Tison, K. Chatterjee, W. C. Miles and C. G. Simon Jr, *J. Biomater. Appl.*, 2013, **27**, 695–705.
5 M. Yeo, C. G. Simon and G. Kim, *J. Mater. Chem.*, 2012, **22**, 21636–21646.
6 K. Chatterjee, A. M. Kraigsley, D. Bolikal, J. Kohn and C. G. Simon, *J. Funct. Biomater.*, 2012, **3**, 173–182.
7 C. G. Simon Jr, J. S. Stephens, S. M. Dorsey and M. L. Becker, *Rev. Sci. Instrum.*, 2007, **78**, 072207.
8 J. M. Holzwarth and P. X. Ma, *Biomaterials*, 2011, **32**, 9622–9629.
9 F. J. O'Brien, *Mater. Today*, 2011, **14**, 88–95.
10 L. Van der Schueren, B. De Schoenmaker, O. I. Kalaoglu and K. De Clerck, *Eur. Polym. J.*, 2011, **47**, 1256–1263.
11 J. Glowacki and S. Mizuno, *Biopolymers*, 2008, **89**, 338–344.
12 N. Duguy, H. Petite and E. Arnaud, *Ann. Chir. Plast.*, 2000, **45**, 364–376.
13 E. H. Groeneveld and E. H. Burger, *Eur. J. Endocrinol.*, 2000, **142**, 9–21.
14 K. Fujimura, K. Bessho, K. Kusumoto, Y. Ogawa and T. Iizuka, *Biochem. Biophys. Res. Commun.*, 1995, **208**, 316–322.
15 P. J. Boyne, R. E. Marx, M. Nevins, G. Triplett, E. Lazaro, L. C. Lilly, M. Alder and P. Nummiloski, *Int. J. Periodont. Restor. Dent.*, 1997, **17**, 11–25.
16 K. Kusumoto, K. Bessho, K. Fujimura, J. Akioka, Y. Ogawa and T. Iizuka, *Br. J. Plast. Surg.*, 1998, **51**, 275–280.

17 Y. Okubo, K. Bessho, K. Fujimura, T. Iizuka and S.-I. Miyatake, *Biochem. Biophys. Res. Commun.*, 2000, **267**, 382–387.
18 K. W. Lee, K. S. Chung, J. H. Seo, S. V. Yim, H. J. Park, J. H. Choi and K. T. Lee, *J. Cell. Biochem.*, 2012, **113**, 2835–2844.
19 H. S. Jang, S. H. Kook, Y. O. Son, J. G. Kim, Y. M. Jeon, Y. S. Jang, K. C. Choi, J. Kim, S. K. Han, K. Y. Lee, B. K. Park, N. P. Cho and J. C. Lee, *Biochim. Biophys. Acta, Gen. Subj.*, 2005, **1726**, 309–316.
20 J. H. Kim, H. Y. Go, D. H. Jin, H. P. Kim, M. H. Hong, W. Y. Chung, J. H. Park, J. B. Jang, H. Jung, Y. C. Shin, S. H. Kim and S. G. Ko, *Cancer Lett.*, 2008, **265**, 197–205.
21 J. S. Shin, Y. M. Park, J. H. Choi, H. J. Park, M. C. Shin, Y. S. Lee and K. T. Lee, *Int. Immunopharmacol.*, 2010, **10**, 943–950.
22 D. S. Lee, G. S. Jeong, B. Li, H. Park and Y. C. Kim, *Int. Immunopharmacol.*, 2010, **10**, 850–858.
23 K. Y. Park, G. O. Jung, K. T. Lee, J. Choi, M. Y. Choi, G. T. Kim, H. J. Jung and H. J. Park, *J. Ethnopharmacol.*, 2004, **90**, 73–79.
24 W. K. Jeon, J. H. Lee, H. K. Kim, A. Y. Lee, S. O. Lee, Y. S. Kim, S. Y. Ryu, S. Y. Kim, Y. J. Lee and B. S. Ko, *J. Ethnopharmacol.*, 2006, **106**, 62–69.
25 J. Choi, B. J. Yoon, Y. N. Han, K. T. Lee, J. Ha, H. J. Jung and H. J. Park, *Planta Med.*, 2003, **69**, 899–904.
26 B. Stevens, Y. Z. Yang, A. Mohandas, B. Stucker and K. T. Nguyen, *J. Biomed. Mater. Res., Part B*, 2008, **85**, 573–582.
27 H. J. Lee, S. H. Ahn and G. H. Kim, *Chem. Mater.*, 2012, **24**, 881–891.
28 G. C. Zhou, Y. Lu, H. Zhang, Y. Chen, Y. Yu, J. Gao, D. X. Sun, G. Q. Zhang, H. Zou and Y. Q. Zhong, *Int. J. Nanomed.*, 2013, **8**, 877–887.
29 K. Y. Lee and D. J. Mooney, *Prog. Polym. Sci.*, 2012, **37**, 106–126.
30 L. Liu, L. Jiang, G. K. Xu, C. Ma, X. G. Yang and J. M. Yao, *J. Mater. Chem. B*, 2014, **2**, 7596–7604.
31 N. J. Song, H. J. Yoon, K. H. Kim, S. R. Jung, W. S. Jang, C. R. Seo, Y. M. Lee, D. H. Kweon, J. W. Hong, J. S. Lee, K. M. Park, K. R. Lee and K. W. Park, *J. Lipid Res.*, 2013, **54**, 1385–1396.
32 G. Kim and W. Kim, *Appl. Phys. Lett.*, 2006, **88**, 233101.
33 J. M. Deitzel, J. Kleinmeyer, D. Harris and N. C. B. Tan, *Polymer*, 2001, **42**, 261–272.
34 M. Chen, P. K. Patra, S. B. Warner and S. Bhowmick, *Tissue Eng.*, 2007, **13**, 579–587.
35 G. Kim, J. Son, S. Park and W. Kim, *Macromol. Rapid Commun.*, 2008, **29**, 1577–1581.
36 H. Yoon, S. H. Ahn and G. H. Kim, *Macromol. Rapid Commun.*, 2009, **30**, 1632–1637.
37 C. Mota, D. Puppi, D. Dinucci, C. Errico, P. Bartolo and F. Chiellini, *Materials*, 2011, **4**, 527–542.
38 A. Martins, S. Chung, A. J. Pedro, R. A. Sousa, A. P. Marques, R. L. Reis and N. M. Neves, *J. Tissue Eng. Regener. Med.*, 2009, **3**, 37–42.
39 N. D. Luong, I. S. Moon, D. S. Lee, Y. K. Lee and J. D. Nam, *Mater. Sci. Eng., C*, 2008, **28**, 1242–1249.
40 S. Bose, M. Roy and A. Bandyopadhyay, *Trends Biotechnol.*, 2012, **30**, 546–554.
41 R. P. Batycky, J. Hanes, R. Langer and D. A. Edwards, *J. Pharm. Sci.*, 1997, **86**, 1464–1477.